Published in final edited form as:
J Biol Chem. 2002 April 12; 277(15): 12879–12890.

The Ordered and Compartment-specific Autoproteolytic Removal of the Furin Intramolecular Chaperone Is Required for Enzyme Activation*

Eric D. Anderson‡, **Sean S. Molloy**, **FranÇois Jean**§, **Hao Fei**, **Satoko Shimamura**, and **Gary Thomas**¶
Vollum Institute, Portland, Oregon 97201

Abstract

The propeptide of furin has multiple roles in guiding the activation of the endoprotease *in vivo*. The 83-residue N-terminal propeptide is autoproteolytically excised in the endoplasmic reticulum (ER) at the consensus furin site, -Arg^{104}-Thr-Lys-Arg^{107} ↓ -, but remains bound to furin as a potent autoinhibitor. Furin lacking the propeptide is ER-retained and proteolytically inactive. Co-expression with the propeptide, however, restores trans-Golgi network (TGN) localization and enzyme activity, indicating that the furin propeptide is an intramolecular chaperone. Blocking this step results in localization to the ER-Golgi intermediate compartment (ERGIC)/cis-Golgi network (CGN), suggesting the ER and ERGIC/CGN recognize distinct furin folding intermediates. Following transport to the acidified TGN/endosomal compartments, furin cleaves the bound propeptide at a second, internal P1/P6 Arg site (-Arg-Gly-Val^{72}-Thr-Lys-Arg^{75} ↓ -) resulting in propeptide dissociation and enzyme activation. Cleavage at Arg^{75}, however, is not required for proper furin trafficking. Kinetic analyses of peptide substrates indicate that the sequential pH-modulated propeptide cleavages result from the differential recognition of these sites by furin. Altering this preference by converting the internal site to a canonical P1/P4 Arg motif (Val^{72} → Arg) caused ER retention and blocked activation of furin, demonstrating that the structure of the furin propeptide mediates folding of the enzyme and directs its pH-regulated, compartment-specific activation *in vivo*.

Following correct folding/assembly, many eukaryotic proteins undergo single or multiple endoproteolytic cleavages during transport through the secretory pathway, resulting in the release of smaller, bioactive products. The proprotein convertases (PCs)[1] are a family of calcium-dependent serine endoproteases that catalyze these cleavages at sites containing doublets or clusters of basic amino acids. The PC family is evolutionarily related to bacterial subtilisin and includes seven members expressed in secretory compartments of mammalian cells (see Refs. 1-4 for reviews).

*This work was supported by National Institutes of Health Grant DK37274. The costs of publication of this article were defrayed in part by the payment of page charges. This article must therefore be hereby marked “advertisement” in accordance with 18 U.S.C. Section 1734 solely to indicate this fact.

‡Recipient of a Tartar Trust fellowship. Current address: Dept. of Cell Biology, Yale University School of Medicine, New Haven, CT 06510.
§Recipient of a Medical Research Council (Canada) fellowship. Current address: Dept. of Microbiology, University of British Columbia, Vancouver, British Columbia VT6 1Z3, Canada.
¶To whom correspondence should be addressed. Tel.: 503-494-6955; Fax: 503-494-4534; E-mail: thomasg@ohsu.edu.

[1]The abbreviations used are: PC, proprotein convertase; TGN, transGolgi network; IMC, intramolecular chaperone; ER, endoplasmic reticulum; mAb, monoclonal antibody(s); β-NGF, β-nerve growth factor; MCA, 4-methylcoumaryl-1-amide; HA, hemagglutinin; Fmoc, *N*-(9-fluorenyl) methoxycarbonyl; RP-HPLC, reversed-phase high performance liquid chromatography; Endo H, endoglycosidase H; ERGIC, ER-Golgi intermediate compartment; CGN, cis-Golgi network; BFA, brefeldin A; CMK, chloromethyl ketone; wt, wild type.

Furin, the most intensively studied member of the PC family, is a type I membrane protein localized primarily to the TGN (5-8). Furin is not statically retained in this compartment, but rather it traffics between two local cycling loops, one at the TGN and the other at the cell surface (9,10). The dynamic trafficking of furin enables it to cleave and activate numerous cellular and pathogen proproteins in both the biosynthetic and endocytic pathways (reviewed in Refs. 1 and 4). Endoproteolysis of these substrates occurs primarily at the consensus furin cleavage site, -Arg-*X*-Lys/Arg-Arg ↓ -, containing a P1 and P4 Arg. However, in some cases at acidic pH, furin cleaves substrates at the motif -Arg-*X*-*X*-*X*-Lys/Arg-Arg ↓ -, in which a P6 Arg is present in place of the P4 Arg (11,12).

Before it can act on proprotein substrates, furin itself must go through a complex process of activation. Furin is translated as an inactive zymogen with an 83-amino acid N-terminal propeptide. Attempts to eliminate or substitute the native furin proregion produced inactive enzyme, suggesting that the furin propeptide may play a critical role in folding and activation (13-15). This is consistent with research that shows that the folding of many evolutionarily unrelated classes of protease (*e.g.* serine-, aspartyl-, cysteinyl-and metalloproteases) is mediated by (typically N-terminal) propeptides that act as “intramolecular chaperones” (IMCs). IMC-mediated folding has been most thoroughly investigated in the secreted bacterial serine endoproteases α-lytic protease and subtilisin. These IMCs apparently increase the folding rate of their cognate protease domains by lowering a specific kinetic barrier very late in the folding pathway (reviewed in Refs. 16-20). IMC propeptides are autoproteolytically excised when their cognate enzymes have only partially folded. In subtilisin, propeptide excision initiates significant conformational changes that result in the loss of hydrophobic surface exposure to solvent (21-23). Although no longer covalently attached, these post-excision conformational changes are mediated by the IMC (22). In the absence of the IMC propeptide, the enzyme folds into an inactive and kinetically stable “molten globule”-like intermediate (16,25). The addition of the propeptide *in trans* causes rapid conversion of this folding intermediate to the native state (16,25,27,28).

Following excision, IMCs remain noncovalently bound to their cognate enzymes, acting as tight binding autoinhibitors (29,30). Crystal structures reveal that the propeptide C terminus occupies the active site of the cognate proteases, whereas the rest of the propeptide is folded into a domain distant from the active site (31-33). Thus, propeptide-mediated inhibition is a result of the propeptide cleavage site sequence sterically occluding the active site (34). The residues at the excision site play a critical role in mediating IMC action, possibly by guiding the folding of the active site (17,35). Because IMCs bind and inhibit their cognate proteases, they must be degraded for enzyme activation. This degradation may be autoproteolytic, as has been proposed for subtilisin (31). IMC degradation leaves the cognate protease locked into the native state, which can be metastable (36), by a large kinetic barrier to unfolding (17).

An IMC function for the furin propeptide is consistent with recent work on the maturation of this endoprotease. The furin propeptide is autoproteolytically excised at -Arg-Thr-LysArg^{107} ↓ - in the ER, and excision is necessary for transport from the early secretory pathway (5, 37-39). However, propep-tide excision alone is insufficient for activation, which requires transport to late secretory pathway compartments (5,38). Studies *in vitro* show that after excision the propeptide remains noncovalently bound to furin, acting as a potent auto-inhibitor ($K_{0.5}$ = 14 nM) (13). Exposure of the inactive furin·propeptide complex to conditions characteristic of the microenvironment of the TGN (mildly acidic (pH 6.0) and calcium-containing (low millimolar)) results in a second cleavage within the propeptide at -Arg$_{70}$-Gly-Val-Thr-Lys-Arg^{75} ↓ -. Internal propeptide cleavage requires both P1 and P6 Arg, suggesting that furin might catalyze this step in a manner analogous to its pH-dependent processing of Lstrates with similar cleavage site motifs. Concomitant with cleavage at Arg^{75}, the propeptide

fragments dissociate from furin, permitting the enzyme to cleave Lstrates *in trans*. These *in vitro* findings suggest that *in vivo* furin undergoes its final activation process within the TGN.

The current model of furin activation, characterized by an orchestrated, multistep process involving excision, internal cleavage, and degradation of the propeptide, poses several questions. Does the furin propeptide function as an IMC? Is the activation of furin *in vivo* linked to dissociation of the autoinhibitory propeptide, and if so, is this event regulated by auto-proteolytic cleavage of the propeptide at the Arg^{75} internal cleavage site? Does the sequence of the internal P1/P6 Arg furin propeptide cleavage site contribute to pH regulated processing and activation? And finally, how are these events linked to trafficking of furin within the secretory pathway? In this study we address these questions and show the role of the furin propeptide in guiding the multistep compartment-specific activation of furin *in vivo*.

EXPERIMENTAL PROCEDURES

Cell Culture—BSC-40 cells were maintained in minimal essential medium (Invitrogen) containing 10% fetal bovine serum (HyClone) and 25 μg/ml gentamicin as described previously (40).

Immunofluorescence—Cells were cultured on glass coverslips and grown to 50-80% confluence prior to use. Cells were fixed in 4% paraformaldehyde, and immunofluorescence analysis was performed as described (5). Primary antibodies were used at the following dilutions: mAb M1 and mAb M2 (FLAG) at 1:50 and 1:100, respectively; the signal sequence receptor peptide rabbit antiserum (kindly provided by T. Rapoport) at 1:200; mAb G1/93 (ERGIC-53, kindly provided by H.-P. Hauri) at 1:250; PA1—062 rabbit antiserum (furin cytoplasmic domain, Affinity Bioreagents) at 1:300; mAb 12CA5 (HA, Roche Molecular Biochemicals) at 1:100; and mAb HA.11 (HA, Covance Research Products) at 1:4,000. Secondary antibodies included IgG_{2b}-specific Texas Redconjugated goat anti-mouse (Fisher) used at 1:400, IgG_1-specific fluorescein isothiocyanate-conjugated goat anti-mouse (Fisher) used at 1:150, and Texas Red-conjugated anti-rabbit (Fisher) used at 1:400.

Pro-β-NGF Processing—Metabolic labeling and immunoprecipitations to assess pro-β-NGF processing were performed as described previously (40). The amount of processed β-NGF and unprocessed pro-β-NGF were quantitated using a PhosphorImager 445 SI (Molecular Dynamics).

Pulse-Chase Analysis of Furin Maturation—Pulse-chase and endoglycosidase H digestions were performed as described (5), except PA1-062 (1:250) was used to immunoprecipitate furin molecules.

Membrane Fractionation and Furin Activity Assays—Crude preparations of cellular membranes were made as described previously (13). Furin activity assays with the resuspended membrane pellets were performed in 100 mM HEPES, pH 7.5, 1 mM 2-mercaptoethanol, 0.5% Triton X-100, and 1 mM $CaCl_2$. Fluorometric assays with Pyr-Arg-ThrLys-Arg-MCA peptide were performed as described (41).

Furin Constructs and Vaccinia Virus (VV) Expression—The HA and FLAG epitope-tagged human furin construct fur/f/ha was generated using fur/f/haΔtc-k in pZVneo (13). The *Bam*HI/*Bam*HI fragment from full-length fur/f in pZVneo was domain-swapped into fur/f/haΔtc-k to restore both the transmembrane and cytoplasmic domains. The furin mutants V_{72}R:fur/f/ha, R_{75}A:fur/f/ha, and fur/fΔpro were based on the *Eco*RI/*Kpn*I fragment of furin in pAlter-1 as a template and generated by single primer mutagenesis using the primers V_{72}R (5′-CTGGCATCGAGGCCGGACGAAGCGGTC), R75A (5′-GTGACGAAGGCCTCCCTGTCG), and PROLO1 (5′-

CTGCTAGCAGCTGATGCTGACTACAAGGACGACGAT). The full-length furin constructs were then generated by ligation into pZVneo:fur/f/ha. Pro/ha was generated by standard PCR from the construct fur/f/ha in pZVneo using the primers N.SS.PRO (5′-GAAGATATCATGGAGCTGAGGCCCTGG-3′) and C.PRO (5′-GTCGATATCTCACCGTTT AGTCCGTCGCTT-3′). All constructs were ultimately cloned into the pZVneo vector to generate recombinant VVs as described previously (42).

Synthesis and Characterization of Internally Quenched Peptides— Peptide synthesis was carried out on an automated peptide synthesizer (Model 431A, Applied Biosystems) using procedures essentially as described previously (43). Following coupling of Fmoc-(3-nitro)-Tyr to the Ala-HMP resin, elongation of the peptide chain was conducted using Fmoc solid-phase peptide chemistry until the last step, whereupon *t*-butoxycarbonyl-anthranilic acid was added. The following side chain protecting groups were used: *t*-butoxycarbonyl for Lys, *tert*-butyl for Ser and Asp, and 2,2,5,7,8-methylchroman-6-sulfonyl for Arg. Peptide derivatives were cleaved from the resin and deprotected by treating the resin for 3 h with reagent K followed by lyophilization and repeated washing with ether. The crude material from each synthesis was purified by RP-HPLC, using first a 300 × 7.80-mm, 10-μm Bondclone semipreparative C_{18} column (Phenomenex, Torrance, CA) followed by separation using an analytical C_{18} column (Vydac, Torrance, CA). The buffer system consisted of an aqueous 0.1% (v/v) trifluoroacetic acid solution and an organic phase consisting of acetonitrile also containing 0.1% trifluoroacetic acid (v/v). The elution was carried out with a linear gradient from 5 to 60% organic phase in 60 min following a 5-min isocratic step at 5% organic phase; the flow rate was either 2.0 ml/min (semipreparative) or 1.0 ml/min (analytical). The elution was monitored on-line by UV absorbency at 225 nm. Each purified peptide analogue was characterized by mass spectroscopy analysis. To determine the site of cleavage by furin, each peptidyl Lstrate was digested for 15 min using 15 nM hFur713t (44) at 25 °C in a total volume of 100 μl. The reactions were stopped by addition of excess EDTA and the cleavage products were separated by RP-HPLC, and their identities established by mass spectroscopy analysis essentially as described previously (41).

Fluorometric Assays and Kinetics—Each fluorogenic Lstrate was stored as a 10 mM stock in dimethyl sulfoxide at —20 °C. For each assay the Lstrate was incubated with secreted, soluble furin in a final volume of 200 μl containing 100 mM bis-Tris/100 mM sodium acetate (pH 6.0 or 7.5) with 1 mM calcium. Incubations for the determination of kinetic constants were conducted with various concentrations (corrected for peptide content) of fluorogenic internally quenched peptide Lstrates for up to 30 min. All assays were performed in duplicate, and the average value is given. Fluorescence measurements were made with a FluoroMax-2 spectrofluorometer equipped with a 96-well plate reader (Instrument SA) using an excitation wavelength set at 320 nm and an emission wavelength set at 425 nm. Some measurements were made with a Hitachi F2000 spectrofluorometer equipped with a cuvette in a final volume of 500 μl, and the assay was conducted for up to 10 min. The values of K_m and V_{max} were determined using a computer-assisted algorithm (Enzfitter). Control studies showed no Lstrate inhibition for any of the fluorogenic peptides at concentrations 10-fold greater than their respective K_m values.

RESULTS

Furin Propeptide Has the Properties of an IMC—To test the possibility that the furin propeptide functions as an IMC, we first examined the requirement of this domain for enzyme activation *in vivo* by analysis of an epitope-tagged human furin molecule, fur/fΔpro (Fig. 1). This furin construct contains an internal deletion of the entire proregion by fusing the furin signal peptide directly to the FLAG-tagged catalytic domain. For comparison, we generated fur/f/ha, a full-length furin construct containing an HA tag within the proregion and a FLAG

tag within the catalytic domain (C-terminal to the propeptide excision site). This double epitope tag strategy permitted simultaneous detection of the furin propeptide and mature domains. Neither epitope tag had detectable effects on the transport and activation of the enzyme (5, 13). Cells expressing either fur/fΔpro or fur/f/ha were analyzed for correct signal/ propeptide removal from each construct as determined by Western blot using FLAG-specific mAbs (Fig. 2A). The mAb M2 cross-reacts with all FLAG-tagged furin molecules, whereas mAb M1 requires the tag at the free N terminus (*i.e*. cleavage of the signal peptide in fur/fΔpro and the propeptide in fur/f/ha, see Fig. 1). The mAb M1 cross-reactivity of the fur/fΔpro and fur/f/ha molecules confirms that the mature proteins possess the same primary amino acid sequences following signal sequence and propeptide (fur/f/ha only) excision (Fig. 2A). Quantitative enzyme assays *in vitro* revealed the importance of the propeptide to furin activity (Fig. 2B). Extracts from cells expressing fur/f/ha displayed robust activity, whereas fur/fΔpro showed no activity above control samples.

The importance of the propeptide for correct furin localization was also revealed by analyses of the immunofluorescence and glycosylation state. Immunofluorescence analysis showed a distinct localization of fur/f/ha and fur/fΔpro in BSC-40 cells (Fig. 2C). Consistent with the previously demonstrated TGN localization of furin (5), fur/f/ha showed a paranuclear staining pattern with both mature domain (mAb M1) and proregion-directed (mAb HA.11) antibodies. By contrast, fur/fΔpro showed an ER-like staining with mAb M1 including the nuclear envelope and a dispersed reticular pattern that overlapped with the signal sequence receptor, an ER marker. Similar results were obtained with a pulse-chase analysis (Fig. 2D). Following a 30-min pulse with ^{35}S-labeled amino acids, the newly synthesized zymogen and mature forms of fur/f/ha were both sensitive to digestion with endoglycosidase H (Endo H), indicating localization to the ER. After a 3-h chase, most mature fur/f/ha migrates as a larger molecular weight, Endo H-resistant band demonstrating transport to late secretory pathway compartments. By contrast, fur/fΔpro remained in a lower molecular weight, fully Endo H-sensitive form, suggesting that the furin propeptide is required for export of the enzyme from the ER. The relatively high recovery of fur/fΔpro during the entire chase period further indicated that its transport was blocked in the early secretory pathway, because normally a significant portion of furin is proteolytically shed upon delivery to the TGN and is secreted from the cell (reduced signal in fur/f/ha chase lanes).

If, as indicated by these results, the furin propeptide functions as an IMC, then co-expression of the propeptide *in trans* with fur/fΔpro should rescue fur/fΔpro from the ER and restore enzymatic activity. To test this possibility, a truncated molecule was generated containing only the furin signal sequence followed by the HA epitope-tagged propeptide (*pro/ha*; see Fig. 1). Cells expressing fur/fΔpro alone or together with pro/ha were incubated with mAb M1 in culture to identify furin molecules recycling from the cell surface. Following fixation, the remaining fur/fΔpro was labeled with mAb M2. Although fur/fΔpro expressed alone or with a control vector did not cycle to the cell surface (as expected based upon its ER localization), co-expression with pro/ha resulted in significant uptake of mAb M1, which gave a punctate, paranuclear stain consistent with TGN localization (Fig. 3A). Thus, pro/ha was able to restore both TGN localization and cell surface cycling of fur/fΔpro. The rescue was not complete because post-fix staining with mAb M2 revealed that some fur/fΔpro remained in the ER (see “Discussion”).

To determine whether pro/ha could also rescue fur/fΔpro activity, we used an *in vivo* pro-β-NGF processing assay. This highly sensitive *in vivo* assay was used as opposed to the comparatively less sensitive *in vitro* peptide Lstrate assay,[2] as the rescue of fur/fΔpro localization to the TGN by pro/ha was incomplete. Parallel plates of cells were co-infected

[2]E. D. Anderson and G. Thomas, unpublished results.

with vaccinia recombinants expressing pro-β-NGF and fur/fΔpro alone or with pro/ha. The cells were incubated with [^{35}S]Met/Cys, and secreted pro-β-NGF products were immunoprecipitated and used to quantify processing efficiency (Fig. 3B). Expression of pro-β-NGF with either pro/ha or fur/fΔpro separately failed to enhance processing above control levels. By contrast, co-expression of pro/ha with fur/fΔpro resulted in significant pro-β-NGF processing. Thus, the furin propeptide expressed in trans can restore both fur/fΔpro activity and trafficking.

The IMC-like properties of the furin propeptide suggested that failure of full-length furin to undergo propeptide excision could result in the accumulation of a furin folding intermediate. To test this prediction, we examined the expression of fur/fD153N, a FLAG-tagged furin construct with an inactivating mutation in the catalytic triad (Asp^{153} → Asn; see Fig. 1). This strategy was based on the finding that active site mutation of the structurally related bacterial Ltilisin blocks propeptide excision but not enzyme folding (23,45). Using Western blotting (Fig. 4A), *in vitro* activity assays (Fig. 4B), and pulse-chase analysis (Fig. 4C), we verified that fur/fD153N fails to undergo propeptide excision and thus cross-react with mAb M1. Similar to fur/fΔpro, the propeptide-containing fur/ fD153N is inactive and remains fully Endo H-sensitive, consistent with an early secretory pathway transport block. In contrast to fur/ fΔpro, however, fur/fD153N displayed a more dispersed punctate staining pattern with a paranuclear component that showed a limited overlap with ERGIC-53, a marker for the ER-Golgi intermediate compartment (ERGIC, Fig. 4D). This limited overlap between fur/fD153N and ERGIC-53 was confirmed by confocal microscopy (data not shown). The significant amount of fur/fD153N that did not co-localize with ERGIC-53 could reflect an unidentified Lcompartment of the ERGIC or the adjacent cis-Golgi network (CGN). Therefore, to examine further the localization of fur/fD153N, cells were treated with brefeldin A (BFA) prior to fixation. In addition to its ability to cause fusion of Golgi and ER membranes, BFA also causes fusion of the ERGIC and CGN membranes (46). Consistent with localization of fur/fD153N to the ERGIC/CGN, BFA treatment caused a nearly complete redistribution of fur/fD153N to punctate ERGIC-53-containing structures (Fig. 4D). This result suggests that failure to excise the propeptide results in a furin folding defect which, unlike fur/fΔpro, permits export from the ER but not from the ERGIC/CGN.

Autoproteolytic Cleavage of the Internal Furin Propeptide Site at Arg^{75}—Once an IMC has served its function in enzyme folding, this autoinhibitory domain must be removed to permit protease activation. In the case of the degradative bacterial Ltilisins, this is achieved via indiscriminate and rapid hydrolysis of the propeptide (reviewed in Ref. 19). By contrast, furin remains inactive following autoproteolytic propeptide excision in the ER (-Arg-Thr-Lys-Arg^{107} ↓ -), due to stable association with the autoinhibitory propeptide ($K_{0.5}$ = 14 nM (13)). *In vitro*, activation of this furin·propeptide complex is concomitant with an internal cleavage of the propeptide at the P1/P6 Arg motif, -Arg-Gly-Val-Thr-Lys-Arg^{75} ↓ -, followed by the dissociation of the cleaved propeptide from furin. Cleavage at this site requires both a P1 and P6 Arg as well as an acidic pH characteristic of the TGN (optimal cleavage at pH 6.0 (13)). Furin cleaves Lstrates with intact P1/P6 Arg motifs selectively at acidic pH (see the Introduction), raising the possibility that the internal propeptide cleavage is autoproteolytic. To test this possibility, we performed a series of biochemical and cell biological analyses to determine whether cleavage at Arg^{75} is indeed autoproteolytic and is required for furin activation *in vivo*.

Initially, the sensitivity of internal propeptide cleavage to furin inhibitors was investigated using an ER-localized furin construct, fur/fΔtc-k (see Fig. 1), that undergoes propeptide excision but remains proteolytically inactive because of the stable association of the inhibitory propeptide at the neutral pH of the ER (13). Detergent-solubilized membrane preparations containing fur/fΔtc-k were made and incubated at pH 6.0 in the absence or presence of two

potent furin inhibitors, decanoyl-Arg-Val-Lys-Arg-CH_2Cl, a nM inhibitor of all PCs (41), and the selective furin inhibitor, α_1-PDX ($K_i$for furin = 0.6 nM, Fig. 5A and Ref. 41). Consistent with autoproteolysis, both inhibitors blocked the internal cleavage of the furin propeptide and formation of the ~6 kDa HA-tagged, N-terminal $Gln^{25} \rightarrow Arg^{75}$ fragment (13). A dilution analysis was also performed to establish whether internal propeptide cleavage was an inter- or intramolecular process. Replicate samples containing fur/fΔtc-k were sequentially diluted (up to 20-fold) and incubated at pH 6.0 for 3 h, during which time furin becomes maximally active *in vitro* (13). Relative furin activity was then determined, and the number of furin active sites measured by titration analysis (Fig. 5B). The observed regression line does not pass through the null point when approaching 0 nM "activable" furin, indicating an intramolecular activation event. However, the rate of activation increases at higher furin concentrations, suggesting an additional intermolecular component. Although the precise *in vivo* concentration of the low abundance endogenous furin is unknown, these results collectively indicate that the enzyme becomes active via a predominantly intramolecular process even at very high local concentrations.

To test directly the hypothesis that autoproteolytic propep-tide cleavage at -Arg-Gly-Val-Thr-Lys-$Arg^{75}\downarrow$- is based on the pH-dependent cleavage site specificity of furin, a kinetic analysis was performed using internally quenched fluorogenic peptide Lstrates corresponding to the sites of propeptide excision (PS-1) and internal propeptide cleavage (PS-2; see Table I). Consistent with the processing of P1/P4 Arg-containing furin Lstrates, the PS-1 peptide had a low μM K_m value at both neutral and acidic pH but was cleaved slightly more efficiently at pH 7.5. By contrast, the P1/P6 Arg-containing PS-2 peptide showed a marked preference for cleavage at pH 6.0. A much larger K_m (23.8 μM) was observed at neutral pH; however, this value was reduced by 3-fold (6.6 μM) at pH 6.0. Moreover, unlike PS-1, cleavage of PS-2 was slightly more efficient at pH 6 than at pH 7.5. These data support a model in which compartment-specific activation of furin is controlled, in part, by different motifs at the two propeptide cleavage sites (see "Discussion"). In addition, the more inefficient cleavage of PS-2 compared with PS-1 may explain, in part, the slower autoproteolysis at Arg^{75} compared with Arg^{107} during furin activation (see below).

The Slow Autoproteolysis at Arg^{75} Is Necessary for in Vivo Furin Activation but Not Trafficking—The kinetics of autoproteolytic cleavage and dissociation of the furin propeptide *in vivo* was determined by pulse-chase, co-immunoprecipitation analysis. Cells expressing fur/f/ha were pulse-labeled with [^{3}H]Arg/Leu and harvested either immediately or following a chase period of increasing time. Furin·propeptide complexes were then immunoprecipitated with mAb M1, resolved by SDS-PAGE, and processed for autoradiography. Dissociation of the propeptide from furin was quantified by liquid scintillation counting of the excised gel bands (Fig. 5C). Following the pulse labeling, 100% of fur/f/ha molecules were associated with propeptide. The chase analysis showed that the fraction of propeptide-associated furin decreased linearly for ~3.5h($t_{½}$ = 105 min) culminating in 50% dissociation. Longer chase times did not reveal further propeptide dissociation (data not shown; see "Discussion"). BFA treatment, which blocks ER to TGN transport, abolished propeptide dissociation from furin, demonstrating a requirement for transit of furin·propeptide complexes to late secretory pathway compartments for activation (Fig. 5C). The slow time course of propeptide dissociation is consistent with the slower cleavage of the PS-2 Lstrate *in vitro* (Table I). Moreover, the inhibition of this step by BFA further indicates a requirement for transport of the furin·propeptide complex to TGN/endosomal compartments for the *in vivo* autoproteolysis at Arg^{75}.

The importance of cleavage at Arg^{75} to furin activation and sorting was examined *in vivo*. Biochemical analyses of the biosynthesis and activation of a furin molecule containing an $Arg^{75} \rightarrow$ Ala Lstitution (R75A:fur/f/ha) showed no effect on the initial ER-localized propeptide excision at Arg^{107}, but this Lstitution still blocked enzyme activation (Fig. 6, A and

B). Despite this block in furin activation, pulse-chase analysis showed the $Arg^{75} \rightarrow Ala$ mutation did not impair transport to the late secretory pathway compartments (Fig. 6C). Moreover, immunofluorescence analyses showed that fur/f/ha and R75A: fur/f/ha displayed very similar staining patterns (Fig. 7, *Control*). The paranuclear staining of both furin mature domains (mAb M1) co-localized with that of their propeptides (HA.11), consistent with the localization of the native and mutated furin·propeptide complexes to the TGN. In addition, a low level of propeptide staining was also detected in the ER of both fur/f/ha- and R75A:fur/f/ha-expressing cells. This ER staining likely represents nascent furin molecules, as it was depleted by a brief cycloheximide chase (data not shown). If, however, the cells were treated for 4 h with cycloheximide prior to fixation and staining, a striking difference between fur/f/ha and R75A: fur/f/ha was observed (Fig. 7, *CHX treated*). Fur/f/ha showed a complete loss of paranuclear propeptide (HA.11) staining, whereas R75A:fur/f/ha maintained prominent propeptide staining that remained co-localized with the mature domain. Consistent with the prolonged co-localization of propeptide and mature domain, co-immunoprecipitation analysis (as described above) revealed that R75A propeptide remained largely associated with the enzyme throughout the chase (~87%, data not shown). These data indicate that dissociation of the propeptide from furin requires the integrity of the Arg^{75} cleavage site. Antibody uptake studies, however, showed indistinguishable staining patterns of internalized mAb M1 for fur/f/ha and R75A:fur/f/ha demonstrating that inhibition of internal propep-tide cleavage had no detectable effect on post-TGN trafficking and recycling (Fig. 7, *M1 Uptake*).

The Sequential Order of Propeptide Cleavages Is Essential for Furin Activation—The slow activation of furin both *in vitro* and *in vivo* is presumably due to an inefficient P1/P6 internal propeptide cleavage at Arg^{75} (see Table I). Therefore, we investigated whether mutating the internal cleavage site to a consensus furin cleavage motif containing a P4 Arg (-Arg-X-Lys/Arg-Arg ↓ -) could accelerate the rate of furin activation. If internal propeptide cleavage in this mutant were efficient at neutral pH, furin might become active in the ER. To test this hypothesis, we first examined the processing kinetics of a fluorogenic peptide Lstrate corresponding to the internal propeptide cleavage site incorporating a P4 Arg (*i.e.* $Val^{72} \rightarrow Arg$) (PS-2:V72R; Table I). The introduction of the P4 Arg resulted in an ~3-fold drop in K_m relative to the native internal cleavage site sequence making it comparable with PS-1. Despite the lower K_m, the PS-2:V72R peptide still showed a pH-dependent effect on the K_m (5.17 μM at pH 7.5 to 1.84 μM at pH 6.0), similar to that seen with PS-2 (~3-fold). In addition to the change in K_m, the efficiency of PS-2:V72R hydrolysis (κ_{cat}/K_m) increased ~30-fold over that observed for PS-2 and ~10-fold over that observed for PS-1.

These kinetic data suggested that cleavage of the internal propeptide site containing the $Val^{72} \rightarrow Arg$ mutation should indeed be more efficient than that of the native propeptide site at neutral pH *in vivo*. Therefore, the effects of the P4 $Val^{72} \rightarrow Arg$ Lstitution on the biosynthesis and activation of an epitope-tagged furin construct, V72R:fur/f/ha, were determined. Surprisingly, V72R:fur/f/ha failed to undergo efficient propeptide excision and remained largely a zymogen that displayed no proteolytic activity *in vitro* against a peptide Lstrate (Fig. 8, A and B). Furthermore, unlike R75A:fur/f/ha, pulse-chase studies showed V72R:fur/f/ha remained predominantly Endo H-sensitive (Fig. 8C), indicating retention in the early secretory pathway. In agreement with the pulse-chase studies, immunofluorescence analysis showed V72R:fur/f/ha was predominantly ER-localized as it co-localized with the signal sequence receptor (Fig. 8D). Interestingly, a small amount of TGN localized, mAb M1-positive (*i.e.* propeptide excised) V72R:fur/f/ha was visible by immunofluorescence (data not shown) and Western blotting (Fig. 8A), indicating that a minor pool of V72R:fur/f/ha did mature normally. Although this pool was not detectable by the *in vitro* activity assay (Fig. 8B), pro-β-NGF processing *in vivo* was slightly enhanced in the presence of V72R:fur/f/ha (data not shown). This suggested that a fraction of the molecules were indeed active. Clearly, however, the majority of V72R:fur/f/ha is inactive, suggesting that the P1/P6 Arg structure of the internal

propeptide cleavage site not only imparts pH dependence to the furin activation process but also is critical for proper IMC function.

Together, these results indicate that V72R:fur/f/ha is unable to transit out of the ER, implying misfolding and retention by the ER quality control system. To test this possibility, the $Val^{72} \rightarrow$ Arg mutation was introduced into fur/f/haΔtc-k to facilitate *in vitro* activation analyses (Fig. 9). We found that the V72R: fur/f/haΔtc-k construct could not be activated in vitro even by limited trypsinolysis, which bypasses the normal pH dependence of propeptide cleavage. This result strongly supports the idea that V72R:fur/f/ha is predominantly misfolded *in vivo* and that the ordered, compartment-specific autoproteolysis of the furin propeptide is necessary for enzyme activation.

DISCUSSION

Furin activation is a multistep process that requires an ordered pair of compartment-specific autoproteolytic propep-tide cleavages to produce the mature active endoprotease. The furin propeptide has several properties of a *bona fide* IMC. First, furin molecules lacking the propeptide are retained in the ER and are enzymatically inactive (Fig. 2). Second, co-expression of the furin propeptide *in trans* rescues both its proteolytic activity and its trafficking to the TGN/endosomal system (Fig. 3). Third, blocking propeptide excision results in an ERGIC/CGN localization, suggesting incomplete folding of furin (Fig. 4). Following the rapid propeptide excision at -ArgThr-Lys-Arg^{107} ↓ - ($t_{½}$ < 10 min) and transport of the furin·propeptide complex to the acidic TGN/endosomal system, the propeptide undergoes a slower (t½ = 105 min) autoproteolytic and predominantly intramolecular cleavage at -Arg-GlyVal-Thr-Lys-Arg^{75} ↓ - (Fig. 5). Like the initial ER-localized propeptide excision, the autoproteolytic cleavage of the furin propeptide at Arg^{75} is required for enzyme activation (Fig. 6). Although propeptide excision is necessary for export from early secretory pathway compartments, blocking internal propeptide cleavage ($Arg^{75} \rightarrow$ Ala) has no apparent effect on TGN/cell surface cycling (Fig. 7). The importance of the sequences comprising either the rapidly cleaved P1/P4 Arg propeptide excision site or the slowly cleaved P1/P6 Arg internal propeptide cleavage sites for directing activation within the variable pH environment of the secretory pathway was suggested by the kinetics of cleavage of synthetic peptides (Table I). Analysis of a peptide Lstrate with the internal site of propeptide cleavage mutated to a consensus P1/P4 Arg furin site ($Val^{72} \rightarrow$ Arg) showed a greatly increased sensitivity to furin at neutral pH. Surprisingly, this mutation *in vivo* resulted in near complete block in activation and ER-localization of furin (Fig. 8). The lack of enzymatic activity of the V72R:fur/f/ha molecule even after trypsinolysis suggested that this mutation causes mis-folding (Fig. 9). Together, these results underscore the importance of an ordered, compartment-specific series of activation steps and provide a rationale for the distinct structures of the excision (Arg^{107}) and internal (Arg^{75}) cleavage sites (summarized in Fig. 10).

Furin Transport Out of the Early Secretory Pathway—Mis-folded or unassembled secretory proteins are retained by the cellular quality control system (reviewed in 48). Although most of these proteins are retained in the ER, some escape the ER and transit to post-ER/pre-Golgi compartments, from which they may be retrieved. Our analysis suggests that the ER and ERGIC/CGN may distinguish furin in different folding states. Apparently misfolded furin constructs (*i.e.* fur/fΔpro and V72R: fur/f/ha) are retained in the ER, perhaps by virtue of chaperone binding. Indeed, preliminary co-immunoprecipitation studies show that fur/fΔpro and V72R:fur/f/ha are selectively associated with BiP.[2] Chaperone binding to fur/fΔpro may account for the incomplete recovery of activity by co-expressed pro/ha (Fig. 3), as BiP may prevent interaction between fur/fΔpro and pro/ha. Alternatively, the lack of an ER retrieval signal in pro/ha may have prevented it from reaching a sufficiently high concentration in the ER to fully rescue furin activity. By contrast, the localization of fur/fD153N to the ERGIC/

CGN suggests that it is partially folded and therefore allowed to progress past the initial ER quality control machinery but not to be transported to late Golgi compartments. We do not know whether fur/fD153N is statically retained or recycles between the ER and ERGIC/CGN or whether fur/fD153N and ERGIC-53, a potential transport receptor (49,50), are physically associated.

The possibility that furin folding/activation intermediates are recognized in a compartment-specific manner may explain the differential localization of furin molecules that are caused by excision site mutations *versus* active site mutations. Both mutations block propeptide excision; however, furin constructs with mutations disrupting their propeptide excision site sequences remain as ER-retained zymogens, whereas the active site mutation causes accumulation in the ERGIC/CGN (Ref. 37 and Fig. 10). This differential localization may be explained by the importance of the propeptide excision site sequence for IMC action as described for α-lytic protease and Ltilisin (29,35) and suggested for Kex2p (51). Thus, mutation of the furin excision site may block the initial ER folding steps, whereas mutation of the catalytic triad may allow these initial steps to occur but block a Lsequent ERGIC/CGN folding event. Indeed, mutation of the catalytic triad of Ltilisin has been shown not to result in misfolding (23,45), suggesting that fur/fD153N may represent the accumulation of a normally occurring, transiently folded intermediate. This idea is consistent with the proposed mechanism of IMC-mediated folding based on studies of α-lytic protease and Ltilisins (reviewed in Refs. 20 and 52). The propeptides of these bacterial enzymes facilitate folding of their cognate proenzymes catalytically by stabilizing a high energy transition intermediate and thereby lowering a kinetic barrier very late in the folding pathway (reviewed in Refs. 17,18, and 20). Hence, the propeptide IMCs of both the mammalian PCs and related bacterial proteases may act as “foldases” in contrast to classical chaperones such as BiP. A similar role for the yeast Kex2p propeptide has also been reported (51).

The TGN/Endosomal System and Furin Activation—A requirement for exposure of the furin·propeptide complex to the acidic TGN/endosomal environment for activation is supported by three findings. First, ER-localized furin·propeptide complexes (*i.e.* fur/fΔtc-k; see Fig. 1) fail to undergo internal propeptide cleavage (13). This step can be promoted, however, by *in vitro* exposure to mildly acidic pH with maximal cleavage occurring at pH 6.0, in good agreement with the observed pH of the TGN (53). Second, peptide Lstrates representing the internal propeptide cleavage site are more efficiently cleaved at pH 6.0 than at neutral pH (Table I). Third, internal cleavage and dissociation can be blocked by treatment with BFA, a compound that inhibits ER to TGN transport (Fig. 5C). Our attempts to inhibit internal propeptide cleavage by treatment of cells with deacidifying agents (*e.g.* chloroquine and bafilomycin A), however, resulted in pleiotropic effects including secondary modifications of furin.[2] The incomplete dissociation of the propeptide from furin during activation was surprising (Fig. 5C). Even at long time points (up to 7 h), propeptide dissociation above ~50% was never observed (data not shown). This may be the result of some furin molecules misfolding due to over-expression, as suggested by the observation that many furin molecules that have undergone propeptide excision remain Endo H-sensitive, indicative of ER retention (Fig. 3). Alternatively, it is possible that over-expression interferes with furin dimerization (54) or an unknown but essential secondary modification. Nonetheless, *in vitro* and *in vivo* data point to the pH of the TGN/endosomal system as key to governing propep-tide cleavage at Arg^{75}.

Compared with the rapid ER-localized propeptide excision ($t_{½}$ < 10 min), the rate of furin activation *in vitro* and *in vivo* is slow ($t_{½}$ = 90 (13) and 105 min (this study), respectively). This difference in efficiency of processing at the first and second propeptide cleavage sites may be explained, at least in part, by the kinetics and pH sensitivity of the representative propeptide Lstrates (Table I). Characteristic of many -Arg-X-Lys/ArgArg ↓ - consensus furin sites,

cleavage of PS-1 (reflecting the site of propeptide excision) is relatively efficient at either neutral or acidic pH (low μM K_m, relatively high κ_{cat}/K_m). By contrast, PS-2 cleavage (reflecting the internal P1/P6 Arg propeptide cleavage site) is slower and pH-sensitive with a 3-fold lower K_m at pH 6.0 (23.8 *versus* 6.6 μM). Moreover, the use of a P6 Arg instead of a P4 Arg at the internal propeptide cleavage site (Arg^{75}) prevents this site from interfering with the cleavage at the propeptide excision site (Arg^{107}). The exquisite pH-controlled recognition of these two sequences is not consistent with the proposal by Bhattacharjya *et al.* (55) that a simple low pH-induced unfolding of the furin propeptide is solely responsible for cleavage at Arg^{75} ↓ (55). This conflict was underscored by the results of altering the internal cleavage site presented in this paper. Introduction of a P4 Arg at the internal cleavage site (Table I) resulted in a sharp drop in K_m coupled with a dramatic increase in $\kappa k_{cat}/K_m$ (~30-fold). Indeed, the κ_{cat}/K_m of PS-2:V72R was nearly 10-fold greater than that of the propeptide excision site peptide, PS-1. In addition, when this Val^{72} → Arg mutation was introduced into furin (V72R: fur/f/ha), it inhibited propeptide excision and resulted in ER retention (Fig. 8).

One explanation for the disrupted activation of V72R:fur/f/ha is based on studies of α-lytic protease and Ltilisin. For both bacterial proteases, the integrity of the propeptide excision site sequence is crucial for IMC activity (29,35). In addition, the Ltilisin propeptide is unstructured, folding only by virtue of interaction with the protease domain (27). Thus, in an unstructured propeptide during early folding times the internal cleavage site of V72R:fur/f/ha may out-compete the excision site for access to the partially folded furin catalytic pocket by virtue of its more favorable kinetic properties (Table I). This inappropriate binding would prevent furin from folding properly, leaving the bulk of the enzyme as a misfolded, ER-retained zymogen (see Fig. 10). In a minority of V72R:fur/f/ha molecules, the propeptide excision site interacts correctly with the active site, resulting in their proper folding (Fig. 8 and data not shown). The scarcity of this species, however, precluded biochemical characterization. Importantly, these data may explain why the site of propeptide excision (-Arg-Thr-Lys-Arg^{107} ↓ -) and the internal site of propeptide cleavage (-Arg-Gly-Val-Thr-LysArg^{75} ↓-) have such different motifs. The amino acids at the site of propeptide excision must bind the active site of the folding furin catalytic domain first in order for the propeptide to obtain structure and exert its IMC action. The nonproductive interaction of the internal cleavage site in an unstructured propeptide is prevented by the unusual P1/P6 Arg motif that conveys a very high K_m in the neutral environment of the ER (Table I). Thus, furin folding and activation is dependent on the sequential interaction of the catalytic pocket with the sites of propeptide excision and internal cleavage-as determined by the relative K_m values of these sites. A potential trivial explanation for our results is that correct folding of the V72R:fur/f/ha propeptide is disrupted and thus is unable to carry out its IMC function. To determine whether this is the case, the complete process of furin folding will need to be reconstituted *in vitro* for biophysical characterization. These studies are currently under way.

Accumulating evidence demonstrates that other PCs undergo propeptide and pH-dependent activation processes (15,56).[2] As all members of the PC family contain clusters of basic amino acids at presumptive propeptide excision and internal cleavage sites (57), our results with furin suggest a general model for activation of the PCs. However, there may be interesting variations found with other family members; for instance, the excision of the PC2 propeptide occurs in the TGN/ secretory granules (58), and internal cleavage is not required for enzyme activation (56). A further intriguing element to PC activation is the essential role of the "P-domain," which was first discovered in Kex2p (24) and later in several other PC members including furin (26). In addition to shedding light on PC activation, the study of furin will facilitate our understanding of IMC-mediated enzyme activation in general. Indeed, the rapidity with which the prokaryotic IMCs are degraded following folding makes the study of late events in this process technically difficult. Therefore, the slow, pH-dependent process of furin autoactivation offers a unique opportunity to study late events in IMC-mediated folding. Thus, studies of furin

have provided insight into the biochemistry and cell biology of IMC-mediated protein folding as well as compartment-specific enzyme activation within the secretory pathway.

Acknowledgments

We are grateful to L. Thomas for expert technical assistance. We thank T. Rapoport and H.-P. Hauri for generously providing reagents. We thank S. Kuman for performing mass spectrometry.

REFERENCES

1. Nakayama K. Biochem. J 1997;327:625–635. [PubMed: 9599222]
2. Seidah NG, Chretien M. Curr. Opin. Biotechnol 1997;8:602–607. [PubMed: 9353231]
3. Steiner DF. Curr. Opin. Chem. Biol 1998;2:31–39. [PubMed: 9667917]
4. Molloy SS, Anderson ED, Jean F, Thomas G. Trends Cell Biol 1999:28–35. [PubMed: 10087614]
5. Molloy SS, Thomas L, VanSlyke JK, Stenberg PE, Thomas G. EMBO J 1994;13:18–33. [PubMed: 7508380]
6. Voorhees P, Deignan E, van Donselaar E, Humphrey J, Marks MS, Peters PJ, Bonifacino JS. EMBO J 1995;14:4961–4975. [PubMed: 7588625]
7. Schafer W, Stroh A, Berghofer S, Seiler J, Vey M, Kruse ML, Kern HF, Klenk HD, Garten W. EMBO J 1995;14:2424–2435. [PubMed: 7781597]
8. Jones BG, Thomas L, Molloy SS, Thulin CD, Fry MD, Walsh KA, Thomas G. EMBO J 1995;14:5869–5883. [PubMed: 8846780]
9. Wan L, Molloy SS, Thomas L, Liu G, Xiang Y, Rybak SL, Thomas G. Cell 1998;94:205–216. [PubMed: 9695949]
10. Molloy SS, Thomas L, Kamibayashi C, Mumby MC, Thomas G. J. Cell Biol 1998;142:1399–1411. [PubMed: 9744873]
11. Chiron MF, Fryling CM, FitzGerald DJ. J. Biol. Chem 1994;269:18167–18176. [PubMed: 8027078]
12. Krysan DJ, Rockwell NC, Fuller RS. J. Biol. Chem 1999;274:23229–23234. [PubMed: 10438496]
13. Anderson ED, VanSlyke JK, Thulin CD, Jean F, Thomas G. EMBO J 1997;16:1508–1518. [PubMed: 9130696]
14. Rehemtulla A, Dorner AJ, Kaufman RJ. Proc. Natl. Acad. Sci. U. S. A 1992;89:8235–8239. [PubMed: 1325651]
15. Zhou A, Paquet L, Mains RE. J. Biol. Chem 1995;270:21509–21516. [PubMed: 7665562]
16. Baker D, Sohl JL, Agard DA. Nature 1992;356:263–265. [PubMed: 1552947]
17. Baker D. Nat. Struct. Biol 1998;5:1021–1024. [PubMed: 9846867]
18. Shinde U, Inouye M. Trends Biochem. Sci 1993;18:442–446. [PubMed: 7904779]
19. Baker D, Shiau AK, Agard DA. Curr. Opin. Cell Biol 1993;5:966–970. [PubMed: 8129949]
20. Baker D, Agard DA. Biochemistry 1994;33:7505–7509. [PubMed: 8011615]
21. Anderson DE, Peters RJ, Wilk B, Agard DA. Biochemistry 1999;38:4728–4735. [PubMed: 10200160]
22. Shinde U, Fu X, Inouye M. J. Biol. Chem 1999;274:15615–15621. [PubMed: 10336458]
23. Eder J, Rheinnecker M, Fersht AR. Biochemistry 1993;32:18–26. [PubMed: 8418836]
24. Gluschankof P, Fuller RS. EMBO J 1994;13:2280–2288. [PubMed: 8194519]
25. Eder J, Rheinnecker M, Fersht AR. J. Mol. Biol 1993;233:293–304. [PubMed: 8377204]
26. Creemers JW, Siezen RJ, Roebroek AJ, Ayoubi TA, Huylebroeck D, Van de Ven WJ. J. Biol. Chem 1993;268:21826–21834. [PubMed: 8408037]
27. Strausberg S, Alexander P, Wang L, Schwarz F, Bryan P. Biochemistry 1993;32:8112–8119. [PubMed: 8347611]
28. Silen JL, Frank D, Fujishige A, Bone R, Agard DA. J. Bacteriol 1989;171:1320–1325. [PubMed: 2646278]
29. Li Y, Hu Z, Jordan F, Inouye M. J. Biol. Chem 1995;270:25127–25132. [PubMed: 7559646]
30. Baker D, Silen JL, Agard DA. Proteins 1992;12:339–344. [PubMed: 1579568]

31. Bryan P, Wang L, Hoskins J, Ruvinov S, Strausberg S, Alexander P, Almog O, Gilliland G, Gallagher T. Biochemistry 1995;34:10310–10318. [PubMed: 7640287]
32. Gallagher T, Gilliland G, Wang L, Bryan P. Structure 1995;3:907–914. [PubMed: 8535784]
33. Sauter NK, Mau T, Rader SD, Agard DA. Nat. Struct. Biol 1998;5:945–950. [PubMed: 9808037]
34. Sohl JL, Shiau AK, Rader SD, Wilk BJ, Agard DA. Biochemistry 1997;36:3894–3902. [PubMed: 9092819]
35. Peters RJ, Shiau AK, Sohl JL, Anderson DE, Tang G, Silen JL, Agard DA. Biochemistry 1998;37:12058–12067. [PubMed: 9724517]
36. Sohl JL, Jaswal SS, Agard DA. Nature 1998;395:817–819. [PubMed: 9796818]
37. Creemers JW, Vey M, Schafer W, Ayoubi TA, Roebroek AJ, Klenk HD, Garten W, Van de Ven WJ. J. Biol. Chem 1995;270:2695–2702. [PubMed: 7852339]
38. Vey M, Schafer W, Berghofer S, Klenk HD, Garten W. J. Cell Biol 1994;127:1829–1842. [PubMed: 7806563]
39. Leduc R, Molloy SS, Thorne BA, Thomas G. J. Biol. Chem 1992;267:14304–14308. [PubMed: 1629222]
40. Bresnahan PA, Leduc R, Thomas L, Thorner J, Gibson HL, Brake AJ, Barr PJ, Thomas G. J. Cell Biol 1990;111:2851–2859. [PubMed: 2269657]
41. Jean F, Stella K, Thomas L, Liu G, Xiang Y, Reason AJ, Thomas G. Proc. Natl. Acad. Sci. U. S. A 1998;95:7293–7298. [PubMed: 9636142]
42. VanSlyke, JK.; Thomas, L.; Thomas, G. Peptidases and Neuropeptide Processing. Smith, AI., editor. 23. Academic Press; San Diego: 1995. p. 45-64.
43. Jean F, Basak A, DiMaio J, Seidah NG, Lazure C. Biochem. J 1995;307:689–695. [PubMed: 7741698]
44. Molloy SS, Bresnahan PA, Leppla SH, Klimpel KR, Thomas G. J. Biol. Chem 1992;267:16396–16402. [PubMed: 1644824]
45. Carter P, Wells JA. Nature 1988;332:564–568. [PubMed: 3282170]
46. Fullekrug J, Sonnichsen B, Schafer U, Nguyen Van P, Soling HD, Mieskes G. FEBS Lett 1997;404:75–81. [PubMed: 9074641]
47. Dayhuff TJ, Gesteland RF, Atkins JF. BioTechniques 1992;13:500–503.
48. Hammond C, Helenius A. Curr. Opin. Cell Biol 1995;7:523–529. [PubMed: 7495572]
49. Nichols WC, Seligsohn U, Zivelin A, Terry VH, Hertel CE, Wheatley MA, Moussalli MJ, Hauri HP, Ciavarella N, Kaufman RJ, Ginsburg D. Cell 1998;93:61–70. [PubMed: 9546392]
50. Vollenweider F, Kappeler F, Itin C, Hauri HP. J. Cell Biol 1998;142:377–389. [PubMed: 9679138]
51. Lesage G, Prat A, Lacombe J, Thomas DY, Seidah NG, Boileau G. Mol. Biol. Cell 2000;11:1947–1957. [PubMed: 10848621]
52. Ellis RJ, Hartl FU. Curr. Opin. Struct. Biol 1999;9:102–110. [PubMed: 10047582]
53. Demaurex N, Furuya W, D'Souza S, Bonifacino JS, Grinstein S. J. Biol. Chem 1998;273:2044–2051. [PubMed: 9442042]
54. Wolins N, Bosshart H, Kuster H, Bonifacino JS. J. Cell Biol 1997;139:1735–1745. [PubMed: 9412468]
55. Bhattacharjya S, Xu P, Xiang H, Chretien M, Seidah NG, Ni F. Protein Sci 2001;10:934–942. [PubMed: 11316873]
56. Muller L, Cameron A, Fortenberry Y, Apletalina EV, Lindberg I. J. Biol. Chem 2000;275:39213–39222. [PubMed: 10995742]
57. Siezen, RJ.; Leunissen, JAM.; Shinde, U. Intramolecular Chaperones and Protein Folding. Shinde, U.; Inouye, M., editors. R. G. Landes Company; Austin, TX: 1995. p. 233-252.
58. Benjannet S, Rondeau N, Paquet L, Boudreault A, Lazure C, Chretien M, Seidah NG. Biochem. J 1993;294:735–743. [PubMed: 8397508]

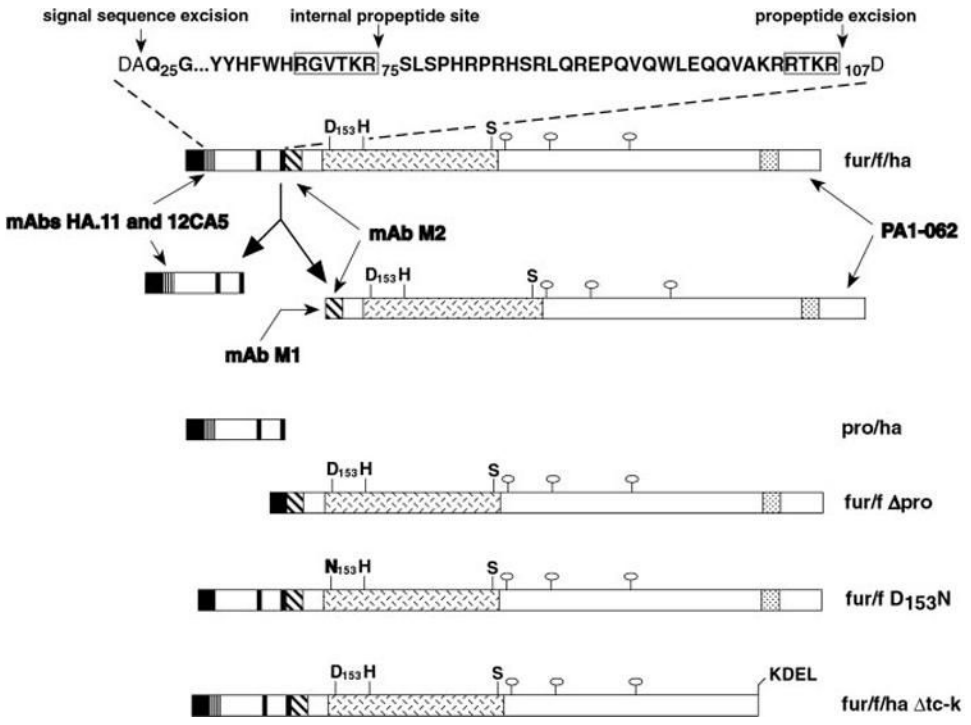

FIG. 1.

Furin constructs. Fur/f/ha, fur/fΔpro, fur/fD153N, fur/f/ha, V72R:fur/ f/ha, and R75A:fur/f/ ha all have the FLAG epitope tag (*diagonal bars*) inserted directly after the propeptide cleavage site, such that the N terminus of the FLAG sequence is exposed upon excision. mAb M2 recognizes either the blocked or exposed forms of the FLAG epitope, whereas mAb M1 requires the FLAG epitope at the free N terminus. In fur/f/ha, pro/ha, V72R:fur/f/ha and R75A:fur/f/ha the HA epitope tag (*vertical bars*) was inserted directly after the signal sequence (black). The HA epitope is recognized by the mAbs 12CA5 and HA.11. The furin cytosolic domain is recognized by the antiserum PA1-062. The Ltilisin-like catalytic domain (*hatch marks*) and the transmembrane domain (*stippled*) are indicated. The catalytic triad residues (Asp, His, Ser) are indicated. "*Lollipops*" denote glycosylation sites. *Thick vertical bars* indicate propeptide cleavage sites. The propeptide excision and internal cleavage motifs are boxed.

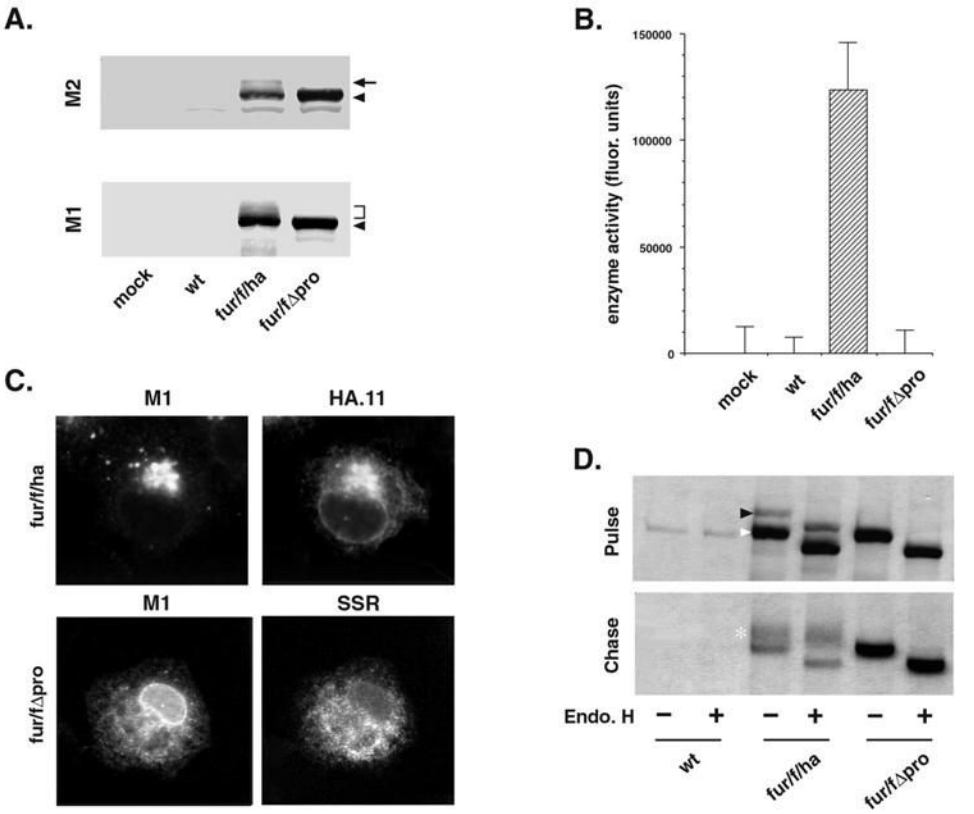

FIG. 2.

Expression and in vitro activity of fur/fΔpro. *A*, membrane preparations from mock infected BSC-40 cells, or BSC-40 cells infected with VV:wt, VV:fur/f/ha, or VV:fur/fΔpro were analyzed by SDS-PAGE followed by immunoblotting, using either mAb M1 or mAb M2. Profurin (*arrow*), propeptide-excised furin (*arrowhead*), and mature sialylated furin (*bracket*) are indicated. *B*, proteolytic activity of the same membrane preparations against Pyr-Arg-Thr-Lys-Arg-MCA. Each *column* represents the average of two samples assayed in duplicate. *Bars* indicate standard deviations. *C*, BSC-40 cells grown on coverslips were infected with VV:fur/f/ha or VV:fur/fΔpro and then fixed at 5 h post-infection and processed for immunofluorescence. Fur/f/ha and fur/f/Δpro mature domains were visualized with mAb M1, and the samples were double-labeled for propeptide (HA.11) or signal sequence receptor (*SSR*). *D*, BSC-40 cells were infected with VV:wt, VV:fur/f/ha, or VV:fur/fΔpro and incubated at 37 °C for 4 h. The cells were pulse-labeled with [^{35}S]Met/Cys for 30 min and chased for 3 h in complete medium with excess cold Met and Cys. Cells were then harvested in mRIPA, and furin was immunoprecipitated with PA1- 062. Immunoprecipitates were incubated in reaction buffer (50 mM sodium citrate pH 6.0, and 0.1% SDS) in the absence (-) or presence (+) of 2.5 milliunits of Endo H. The digested samples were resolved by 8% SDS-PAGE and processed for fluorography. Furin zymogen (*black arrowhead*), mature furin with an excised propeptide (*white arrowhead*), and sialylated furin (*white asterisk*) are indicated.

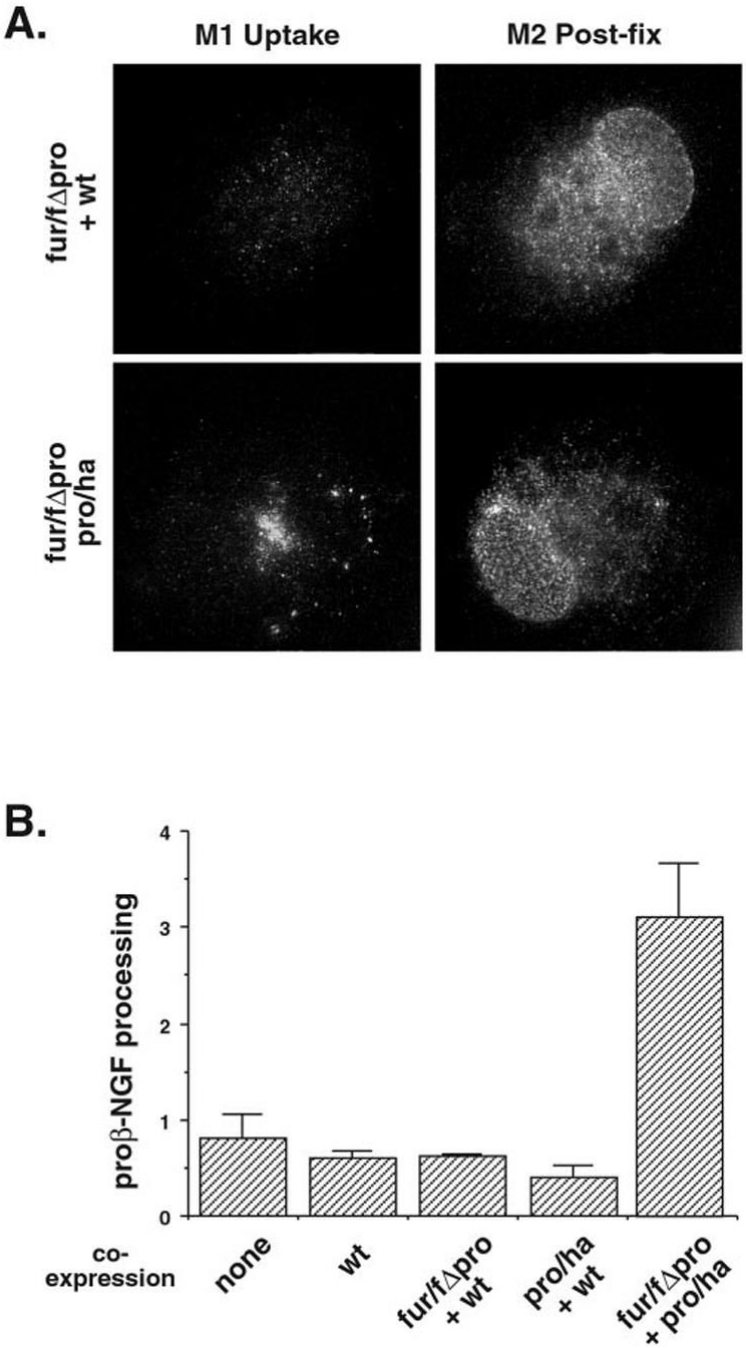

FIG. 3.

Rescue of fur/fΔpro activity and localization by propep-tide *in trans*. *A*, replicate plates of BSC-40 cells grown on coverslips were infected with VV:fur/fΔpro and VV:wt or VV:pro/ha and mAb M1 (30 μg/ml) added to the medium to label mature furin cycling to the cell surface. At 5 h post-infection, the cells were then fixed, permeabilized, and incubated with mAb M2 to detect the remaining furin. mAb M1 and mAb M2 were visualized with isotype-specific secondary antibodies. *B*, replicate plates of BSC-40 cells were infected with either VV:mNGF alone or with additional recombinant viruses as indicated. The signal from the precursor (proβ-*NGF*) and product (β-NGF) were quantitated, and the ratio of product to precursor

determined. Each reading represents the average of two separate samples. *Bars* indicate standard deviations.

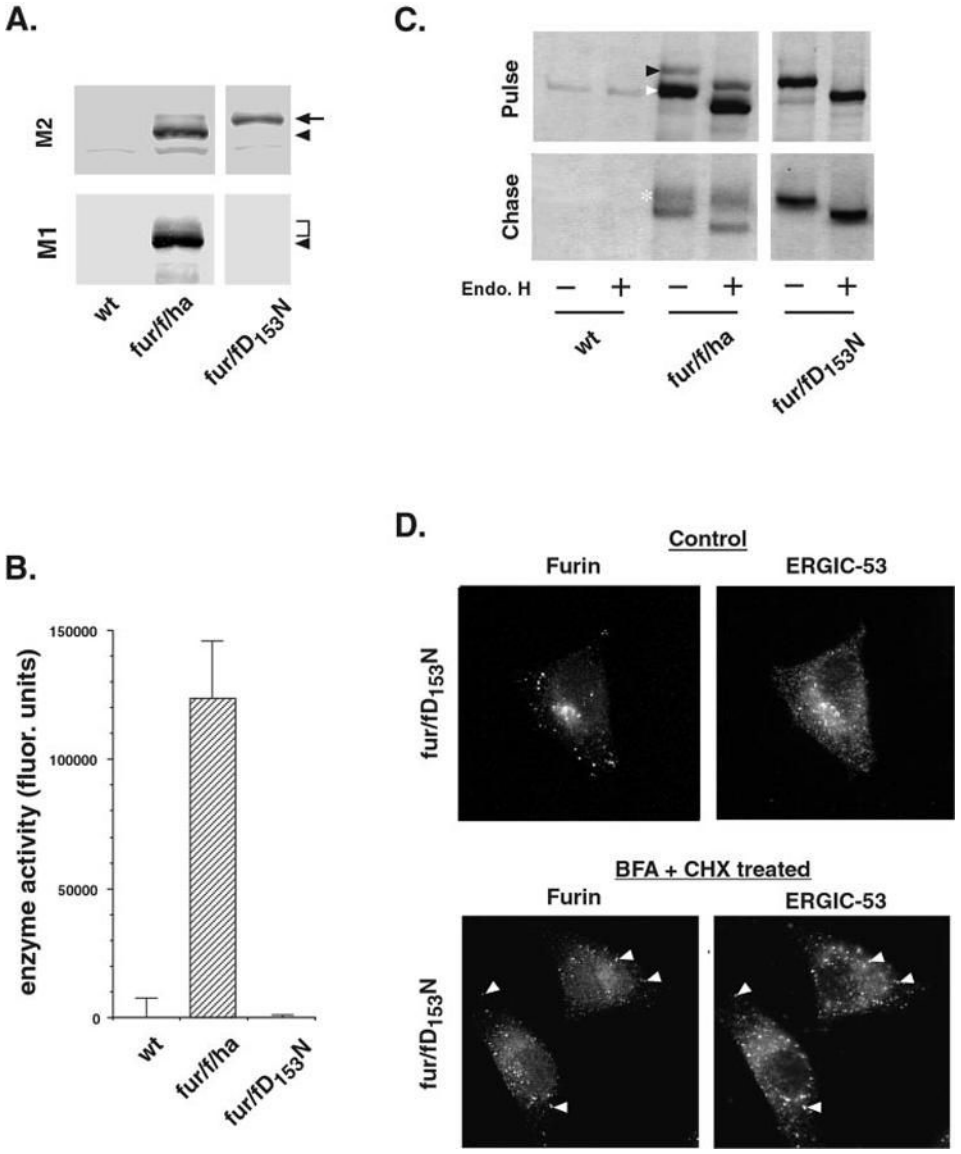

FIG. 4.

Retention of fur/fD153N in the early secretory pathway. *A*, membrane preparations from mock-infected BSC-40 cells or cells infected with VV:wt, VV:fur/f/ha, or VV:fur/fD153N were analyzed by Western blot with mAb M1 and mAb M2. *B*, proteolytic activity of the same membrane preparations. Data are the average of two samples assayed in duplicate. *Bars* indicate standard deviations. *C*, replicate plates of BSC-40 cells were infected with VV:wt, VV:fur/f/ha, or VV:fur/fD153N, pulse-labeled, and chased as described in Fig. 2, and the immuno-precipitates were analyzed by SDS-PAGE and fluorography. *D*, BSC-40 cells were infected with VV:fur/fD153N and incubated at 37 °C for 5 h. In some cases, brefeldin A and cycloheximide (both at 10 μg/ml) were added for the final 2 h prior to fixation. Following fixation, the cells were permeabilized and incubated with PA1- 062 (*Furin*) and mAb G1/93 (*ERGIC-53*) followed by visualization with species-specific secondary antibodies. *Arrowheads* mark examples of structures containing both fur/fD153N and ERGIC-53.

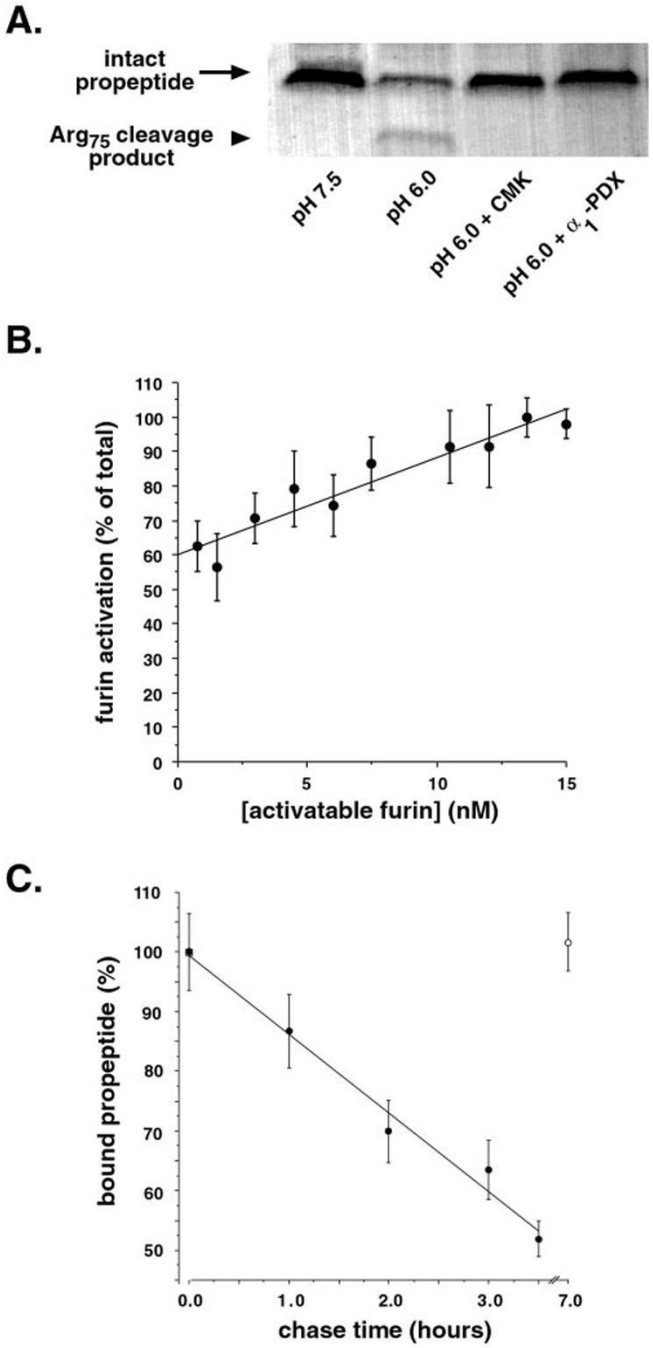

FIG. 5.

Autoproteolytic, intramolecular activation of furin. BSC-40 cells were infected with either VV:wt or VV:fur/fΔtc-k. At 16-18 h post-infection the cells were harvested, and membrane preparations were resuspended in pH 6.0 or 7.5 activation buffer as indicated (10 mM bis-Tris, pH 6.0/pH 7.5, with 5 mM $CaCl_2$ and 1mM βME). In A, 200 μM α_1-PDX or 200 μM decanoyl-Arg-Val-Lys-Arg-CMK were added prior to incubation at 30 °C for 3 h as indicated. Following incubation, the samples were analyzed for the propeptide by Western blot using the anti-HA mAb 12CA5. The intact propeptide (*arrow*) and cleaved ~6-kDa HA-tagged N-terminal propeptide fragment (*arrowhead*) are indicated. In *B*, samples were diluted in pH 6.0 activation

buffer on ice and Lsequently incubated at 30 °C for 3 h. Following incubation, furin activity was determined against the pyr-Arg-Thr-Lys-Arg-MCA Lstrate. Background activity from VV:wt-infected cells was Ltracted from that of VV:fur/fΔtc-k infected cells, and relative activity was calculated. The amount of active furin in the membrane preparation was determined by titration with decanoyl-Arg-Val-Lys-Arg-CMK. The data points indicate the mean of five separate experiments. Bars indicate standard deviation. In *C*, BSC-40 cells were infected with VV:fur/f/ha or VV:R75A:fur/f/ha, incubated for 4 h at 37 °C, and then pulse-labeled for 30 min with 100 μCi each of [^{3}H]Arg and [^{3}H]Leu. The cells were refed with serum-free defined medium (MCDB202) (5) containing excess cold Arg and Leu and harvested after the indicated chase times in TX/Ca^{2+} buffer (50 mM Tris-HCl, pH 8.0, 150 mM NaCl, 1% TX-100, and 1 mM $CaCl_2$) supplemented with 10 μM dec-Arg-Val-Lys-Arg-CMK. Furin was immunoprecipitated with mAb M1 and resolved on a 15% SDS-PAGE peptide gel (47) that was processed for autoradiography. Furin and propeptide bands were excised, dissolved in Solvable (Packard Biosciences), and counted in Hionic Fluor LSC mixture (Packard). The relative propeptide signal is shown as a percentage of the furin signal. The labeling and chase incubations were conducted either in the absence (*closed circles*) or presence (*open circles*) of BFA (10 μg/ml). The experiments were repeated either 10 or 3 times in the absence or presence of BFA, respectively, and *error bars* indicate standard error of the mean.

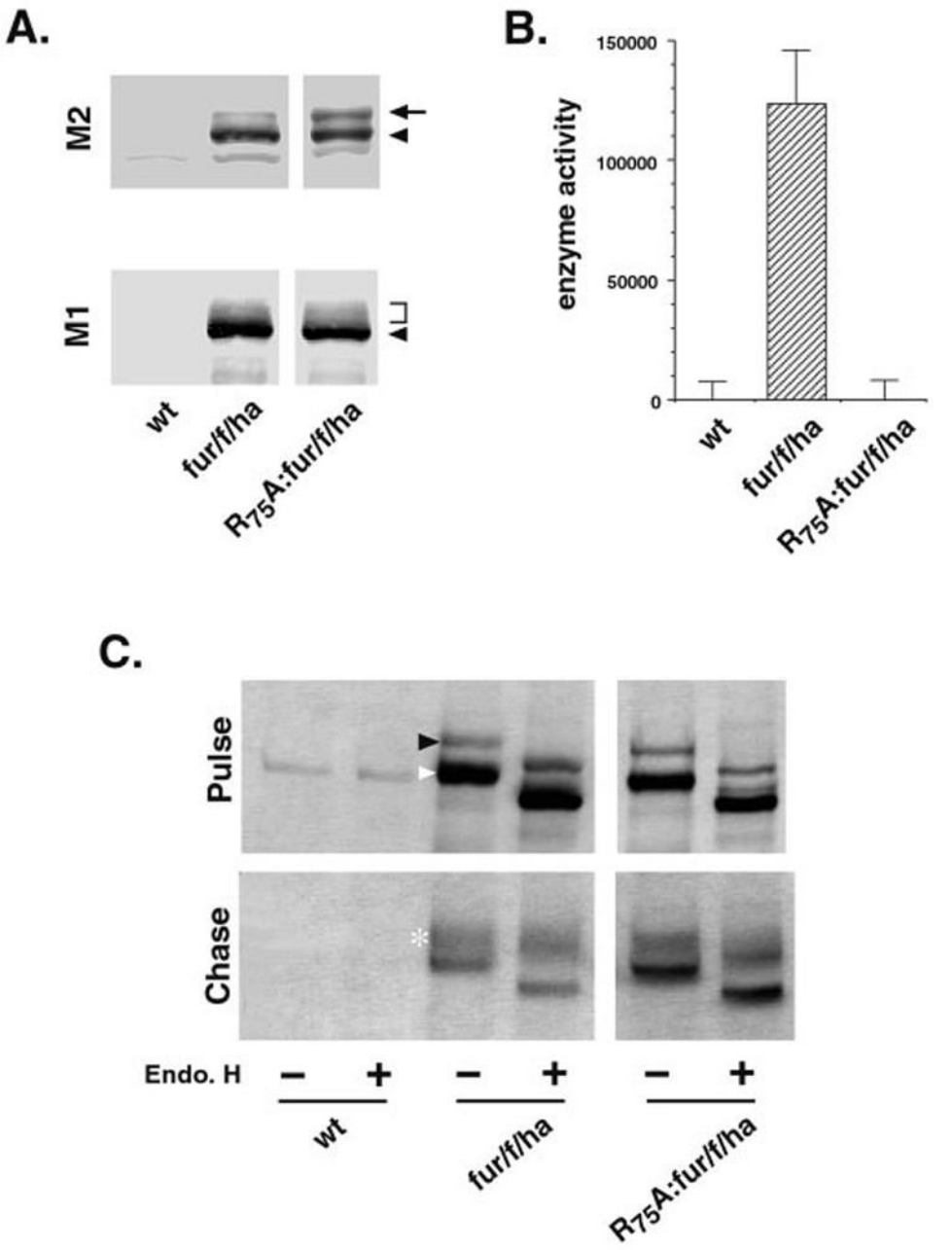

FIG. 6.

Expression and activity of R75A:fur/f/ha. BSC-40 cells infected with VV:wt, VV:fur/f/ha, or VV:R75A:fur/f/ha were processed for Western analysis (*A*), *in vitro* activity assays (*B*), and pulse-chase analyses (*C*) as described in Fig. 2.

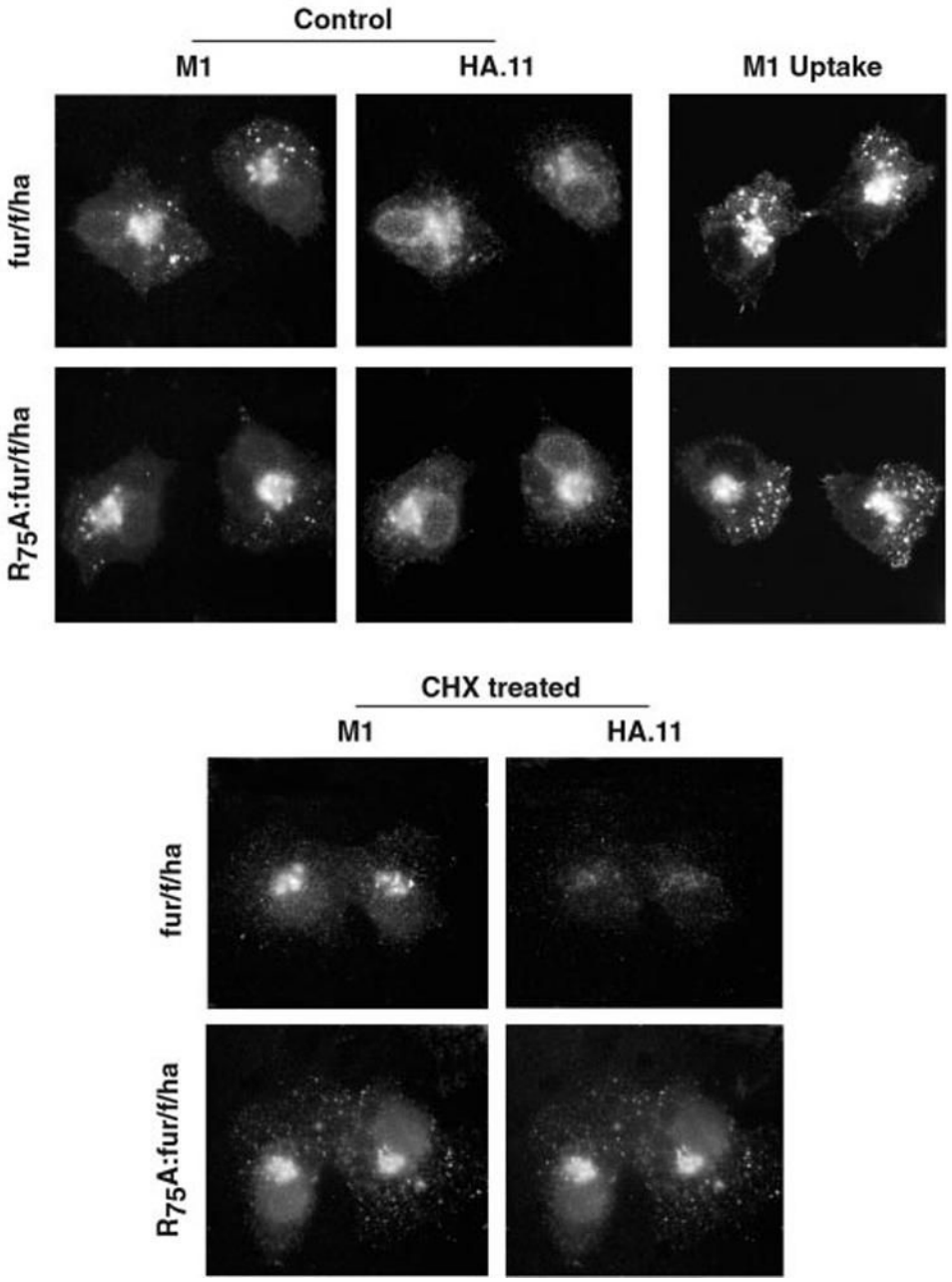

FIG. 7.

Furin·propeptide localization and propeptide dissociation. BSC-40 cells grown on glass coverslips were infected with either VV:fur/f/ha or VV:R75A:fur/f/ha and incubated at 37 °C. Where indicated (*CHX treated*), cycloheximide (10 μg/ml) was added at 2 h post-infection. At 6 h post-infection, the cells were fixed, permeabilized, and incubated with mAb M1 to detect furin mature domain and with HA.11 to detect propeptide; they were visualized with isotype-specific secondary antibodies. In some samples, mAb M1 was added to the culture medium (30 μg/ml) and incubated for an additional hour to label furin molecules recycling from the cell surface prior to fixation (*M1 Uptake*).

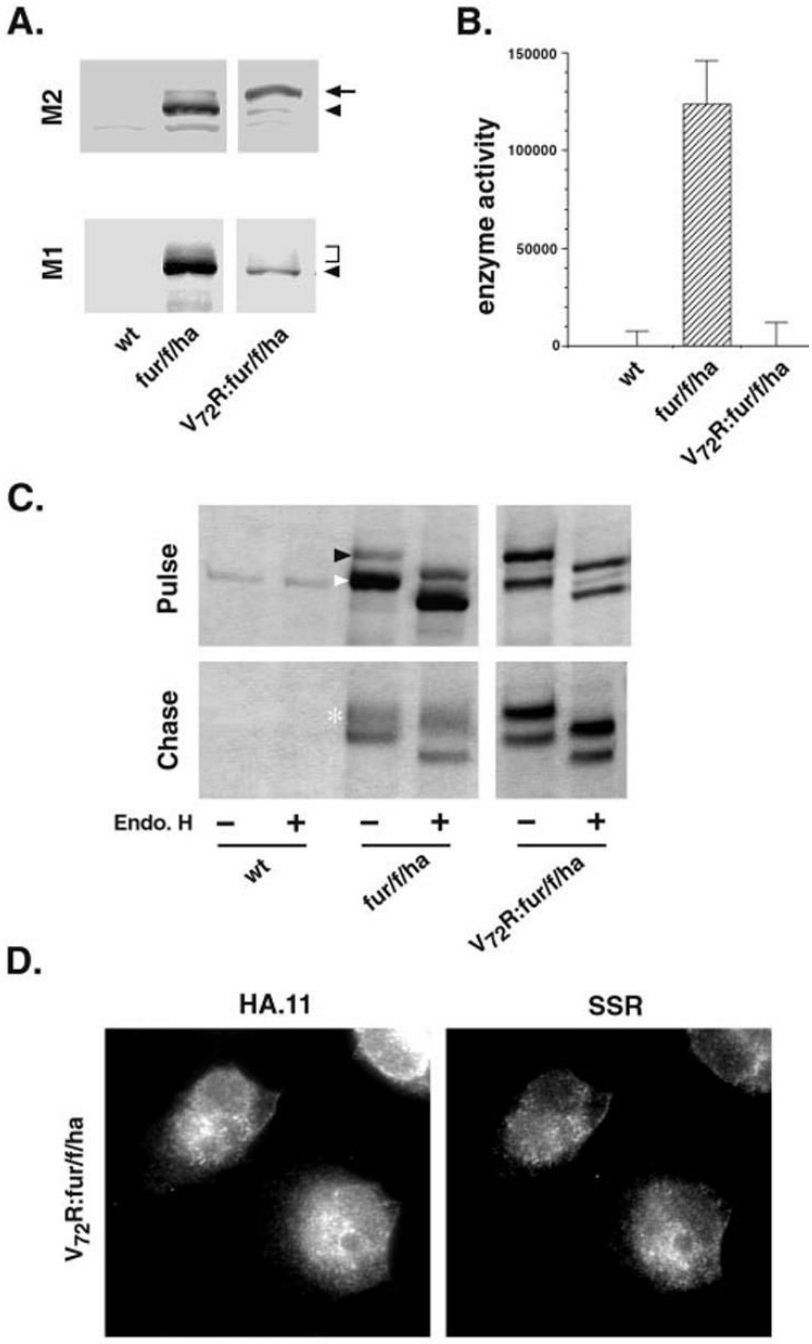

FIG. 8.

V72R:fur/f/ha expression, activity, and localization. BSC-40 cells infected with VV:wt, VV:fur/f/ha, or V72R:fur/f/ha were processed for Western analysis (*A*), in vitro activity assays (*B*), and pulse-chase studies (*C*) as described in Fig. 2. Profurin (*arrow*) and propeptide-excised furin (*arrowhead*) are indicated. *D*, BSC-40 cells infected with VV:V72R:fur/f/ha were fixed after 5 h of incubation at 37 °C and then permeabilized and incubated with mAb HA.11 to detect furin and also with an anti-signal sequence receptor antiserum (*SSR*).

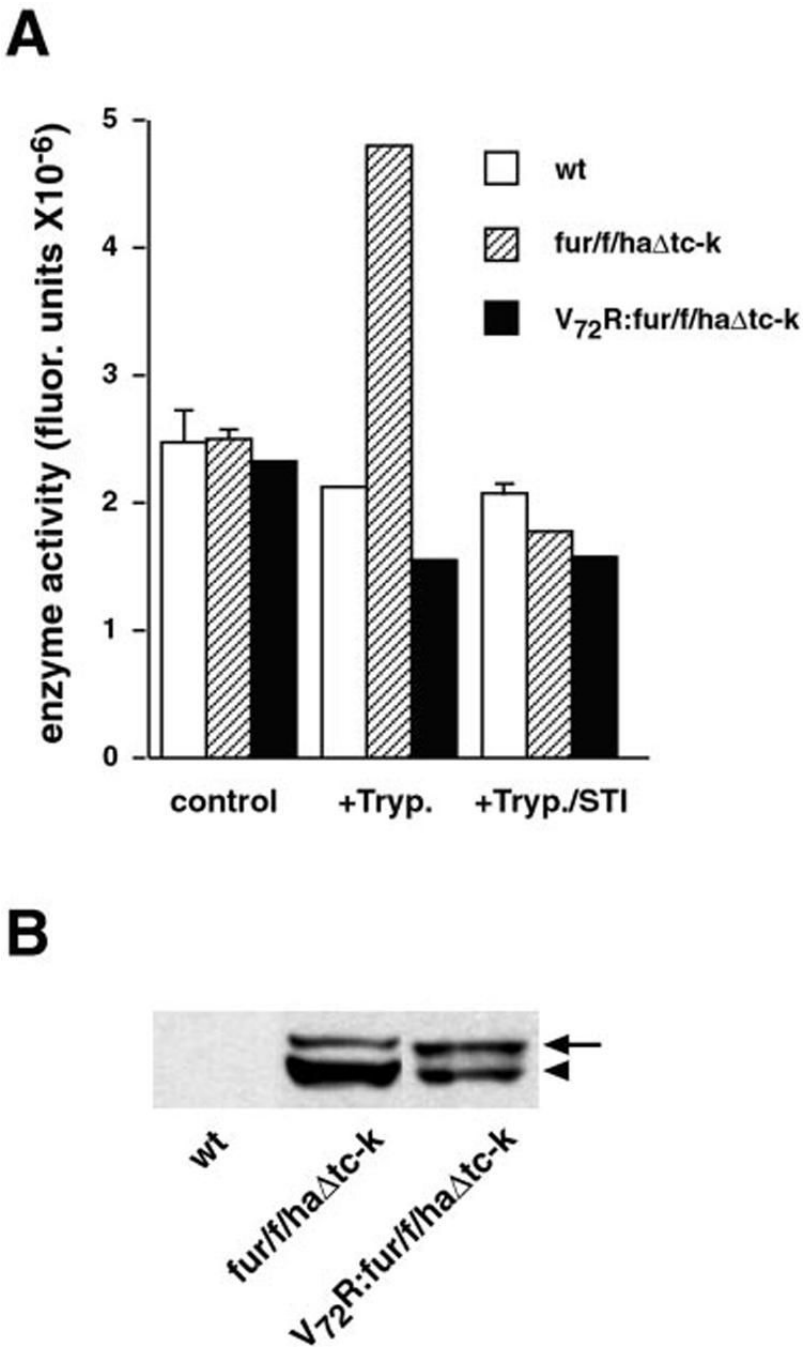

FIG. 9.

***In vitro* activation of furin *versus* V72R mutant**. *A*, BSC-40 cells infected with VV:wt, VV:fur/f/haΔtc-k, or V72R:fur/f/haΔtc-k were harvested, and membrane preparations were resus-pended in activation buffer and incubated at 30 °C in the presence of trypsin (+*Tryp*.) or trypsin and soybean trypsin inhibitor (+*Tryp./STI*) as described (13). Following the activation step, furin activity in each sample was determined using peptide Lstrate. *B*, an equivalent aliquot of each membrane sample was analyzed by Western blot using mAb M2 to monitor expression and processing of the furin constructs.

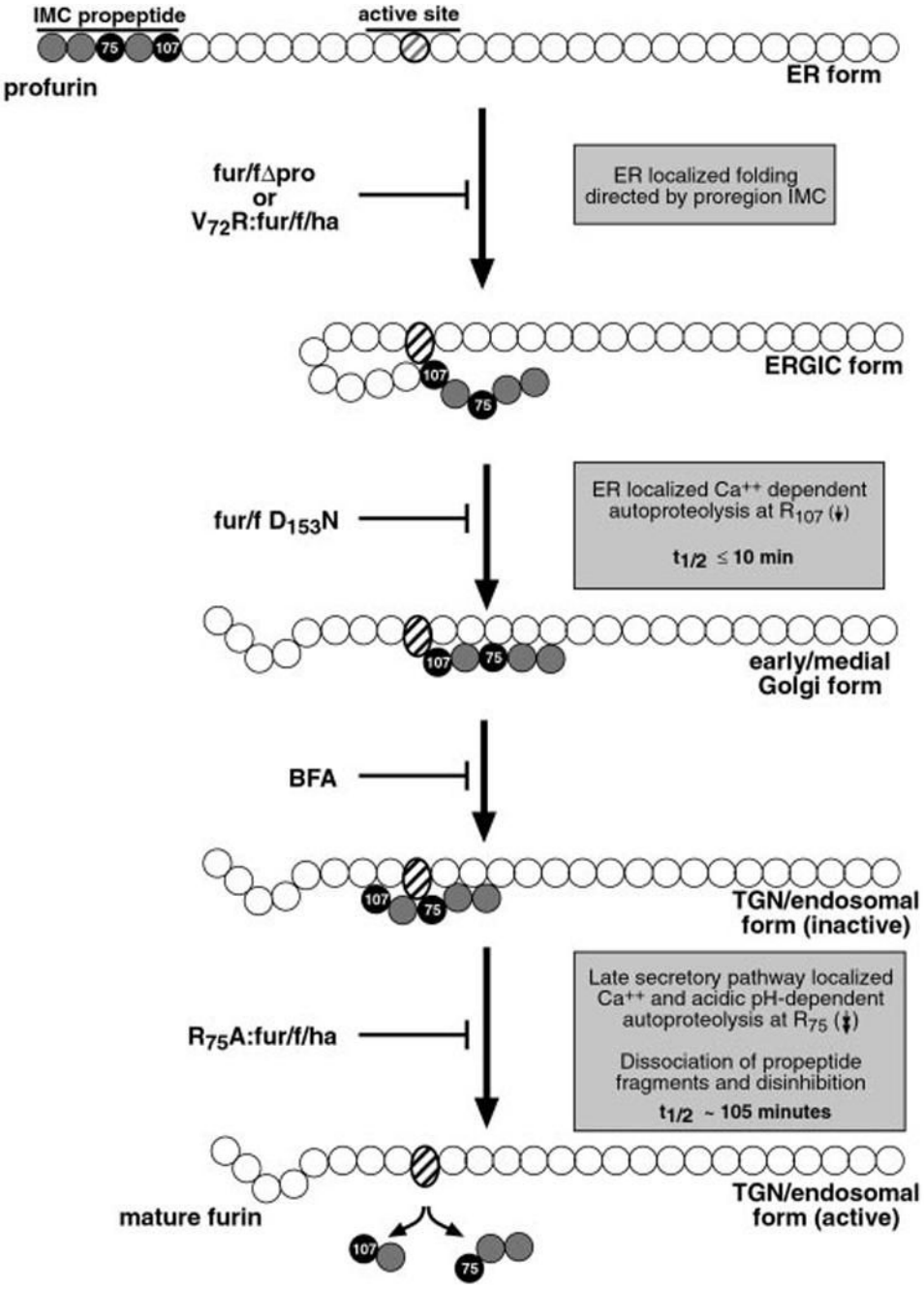

FIG. 10.

Summary of furin activation. Following translation and signal sequence removal, the propeptide acts as an IMC to facilitate folding of the unstructured catalytic domain (*gray-striped circle*) into the active conformation (*black-striped oval*). This process is blocked by deletion of the proregion (*fur/fΔpro*) or by introduction of a canonical P1/P4 Arg furin consensus sequence at the site of internal proregion cleavage (*V_{72}R:fur/f/ha*), resulting in accumulation of misfolded furin molecules unable to exit the ER. The mutated internal cleavage site apparently out competes the native Arg^{107} excision site for binding to the catalytic center. However, the aberrantly bound propeptide fails to correctly fold the profurin molecule (*inset*). After the initial ER folding events, furin undergoes autoproteolytic intramolecular

excision of the propeptide at Arg^{107}. The propeptide, however, remains associated with the mature domain functioning as a potent autoinhibitor *in trans* during transport to the late secretory pathway. Propeptide excision can be blocked by inactivating furin (*fur/fD$_{153}$N*) and results in accumulation of an apparent folding intermediate in the ERGIC/CGN. Following propeptide excision, the inactive furin·propeptide complex transits to late secretory compartments (TGN/endosomes) where the relatively acidic pH promotes autoproteolytic, intramolecular cleavage of the propeptide at a second, internal site, Arg^{75}. The Arg^{75} cleavage is followed by a rapid dissociation of the propeptide fragments and disinhibition of furin. These final activation steps can be blocked by either preventing transport to late secretory compartments (*BFA*) or by eliminating the internal furin cleavage site (*e.g.* $Arg^{75} \rightarrow$ Ala in R75A:fur/f/ha). Blocking the internal cleavage of the propeptide at Arg^{75} results in stabilization of the furin·propeptide complex and prevents activation of furin without altering its trafficking in the TGN/endosomal system.

TABLE I

Peptidyl substrates

	P7 P6 P5 P4 P3 P2 P1 P1′ P2′	pH	K_m	k_{cat}	k_{cat}/K_m	k_{cat}/K_m
			μM	s^{-1}	$s^{-1}M^{-1}$	*Rel*.
PS-1	Abz-Ala-Lys-Arg-Arg-Thr-Lys-Arg↓-Asp-Val-Tyr (NO_2)-Ala	7.5	1.99	1.90	9.58×10^5	1.000
		6.0	1.62	1.03	6.34×10^5	0.611
PS-2	Abz-His-Arg-Gly-Val-Thr-Lys-Arg↓-Ser-Leu-Tyr (NO_2)-Ala	7.5	23.75	6.37	2.68×10^5	0.279
		6.0	6.59	2.92	4.43×10^5	0.462
PS-2:V72R	Abz-His-Arg-Gly-Arg-Thr-Lys-Arg↓-Ser-Leu-Tyr (NO_2)-Ala	7.5	5.17	41.05	7.94×10^6	8.289
		6.0	1.84	16.63	9.04×10^6	9.439